

URBAN THERMODYNAMICS

Innovation Park

AUTHORS

CHRISTINA SCHMID, SCIPER : 345654
HANA WERMEILLE, SCIPER : 340835
ANDREA MONTONERI SCIPER : 344559
PABLO VALLBONA, SCIPER : 339935
SOORYA PASUPATHY, SCIPER : 316467

PROF. DOLAANA KHOVALYG & PROF. KUN LYU



Summary

1	Introduction	1
2	Site Analysis	1
2.1	Site description	1
2.2	Modeling of the site	2
2.3	Simulation of the base case	3
3	Urban Microclimate Exploration	6
3.1	Ground: Light Concrete	6
3.1.1	Selected mitigation & hypothesis	6
3.1.2	Simulation results	7
3.1.3	Discussion	7
3.2	Ground: Clay Soil	8
3.2.1	Selected mitigation & hypothesis	8
3.2.2	Simulation results	9
3.2.3	Discussion	9
3.3	Building Alteration: Height	10
3.3.1	Selected mitigation & hypothesis	10
3.3.2	Simulation results	11
3.3.3	Discussion	12
3.4	Building Alteration: Shape	12
3.4.1	Selected mitigation & hypothesis	12
3.4.2	Simulation results	13
3.4.3	Discussion	14
3.5	Water Body	14
3.5.1	Selected mitigation & hypothesis	15
3.5.2	Simulation results	15
3.5.3	Discussion	16
3.6	Vegetation: Surface Greenings	16
3.6.1	Selected mitigation & hypothesis	17
3.6.2	Simulation results	17
3.6.3	Discussion	18
3.7	Vegetation: Removal of Trees	19
3.7.1	Selected mitigation & hypothesis	19
3.7.2	Simulation results	19
3.7.3	Discussion	20
4	Integrated Microclimate Solution	21
4.1	Simulation results	21
4.2	Discussion	22
5	Conclusion	23
6	Annex	25
6.1	Visit of the site	25
6.2	Model of the site	25

1 Introduction

The world's growing population tends to be more urban, and this constant growth also brings its share of challenges. We observe major changes in urban environment, such as densification, pollution, increase of anthropogenic heat release, all of which profoundly impact the thermal behavior of cities. Phenomenon such as thermal discomfort, urban heat island (UHI) effect, and prolonged and delayed heatwave are becoming critical issues in urban design and must not be underestimated.

This report aims to analyze the thermal behavior of a specific urban site through several points. First, a detailed description of the site will be provided, followed by the development of a digital model. This model will give an insight on the thermal behavior of the site through a simulation and an analysis of several performance indexes. The findings will also serve as a basis for comparing potential improvements to the site by modifying urban elements. Lastly, a generalized upgrade will be proposed incorporating all insights gained through the study.

2 Site Analysis

The first part of our study will be the analysis of the actual site. The analysis was made with different approaches, one by visiting the site and observing some of its features and a second one by modeling and performing a simulation of the site's microclimate on the software ENVI-met.

2.1 Site description

The initial phase of our study involved conducting an on-site visit to collect data and gain a firsthand understanding of the location. The site visit followed a predefined itinerary, as shown in Figure 1, during which we stopped at seven designated points to collect data. At each stop, relevant information was recorded in a structured grid: presence of natural elements, ground cover material; surrounding building material, surrounding building height; anthropogenic heat source, aspect ratio, sky view factor, shading sources. The information gathered can be found in Annex 6.1.

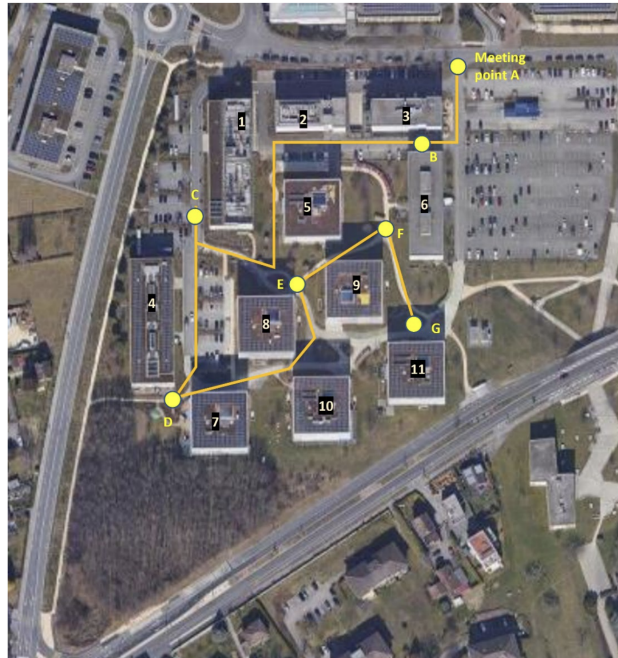


Figure 1: Itinerary of the visit with the different stops

We objectively categorized it as a LCZ 5 type of landscape as it contains some medium building and some green spaces. We see from the layout of the buildings, that there is not a clear urban canyon formed. This layout may help to minimize heat accumulation during hot periods. However, it might not provide sufficient shade when required. Nevertheless, as the area is primarily intended for passing through rather than for prolonged stays, this is not a major concern. We also estimated the areas' fractions such as :

- Building plan area fraction $\lambda_b = \frac{A_b}{A_t} = 40 \%$,
- Vegetated plan area fraction $\lambda_v = \frac{A_v}{A_t} = 40 \%$,

- Impervious plan area fraction $\lambda_i = \frac{A_i}{A_t} = 20 \%$.

An interesting aspect of the Innovation park is the presence of vegetation. It can be found mainly around the site but most importantly in between the buildings. In fact, numerous bushes, flowers, grass, and trees can be observed along the various paths. This can be a big advantage to lower the temperature, create shadow and even produce cleaner air. Regarding the energy balance, the presence of the vegetation can reduce the radiation absorption, increase evapotranspiration and minimize heat storage.

Other interesting features to highlight are the buildings' materials. We observed the extensive use of concrete, characterized by a high thermal capacity, a low albedo, and a moderate conductivity. Therefore, it will absorb a lot of heat during the day and slowly release it during the night retaining a lot of heat in the urban environment which is not very good. Regarding thermal comfort, the use of concrete is less than ideal, as it contributes to increased air and surface temperatures. Its heat storage capacity will in addition produce a delayed heat wave, which produce high temperature even during cooler periods. In addition to concrete, steel is also commonly present in the buildings. It absorbs significant solar radiation and releases it as heat, contributing to increased net radiation in urban environments.

Lastly we want to highlight the source of the anthropogenic heat. During our observations, we noticed that the main source, apart from the building use (light, cooling, heating), are the people as cars are not very present inside the Innovation Park, just some small parking and very few roads. This aspect is beneficial for maintaining cleaner air with less pollution. Additionally, prioritizing pedestrians over cars makes sense since human bodies produce less anthropogenic heat compared to vehicles. However, this analysis holds true only for the park itself. Just outside, there is a large parking lot and two major roads with significant traffic, which could affect the park's energy balance by generating heat flows nearby.

[Climate analysis and material aspects are missing.](#)

2.2 Modeling of the site

The next step of the study was to create a digital model of the site. This will allow us to do simulations giving us more in depth information concerning the thermal behavior of the site. The simulations are done on the software ENVI-met .

The first step is to create a model of the site respecting the layout of the Innovation Park. Some simplification were made as the model cannot recreate the exact reality. Therefore, we have four different type of ground materials as we can see on Figure 2 : sandy loam, concrete pavement (light), concrete pavement (dark), asphalt. We also have vegetation with some bushes and trees.

However, the position, height, shape and number of buildings in the model are true to reality. But regarding the materials of the roofs and the walls, the buildings have been separated into three categories as seen on the final 3D model on Figure 3. The walls and roofs are composed of a series of 3 or 4 layers which can be found in Tables 1, 2 & 3 in Annex 6.2 (note that the first layer is the exterior one).



Figure 2: Soil repartition : sandy loam in khaki, concrete pavement (light) in bright white, concrete pavement (dark) in white, asphalt in black

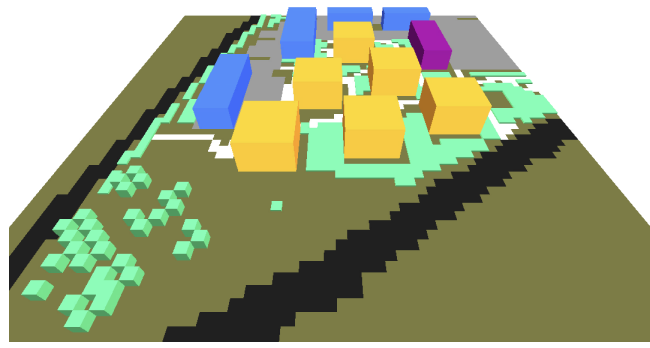


Figure 3: 3D model of the Innovation Park (Buildings A in blue, B in yellow and C in purple)

2.3 Simulation of the base case

Now that the model has been developed, we can run a simulation to gain insights into the site's behavior which will also serve as a basis for comparison for the further study. The simulation reflects the conditions of August 18th, 2021. For the remainder of the study, we have decided to consistently use the results from 2 p.m., as it represents a critical time of day and when radiation emission is at its peak.

The first graph extracted from the simulation result is the sky view factor (Figure 4). As expected from the visit, for the majority it is relatively high since we have medium height buildings and a lot of open spaces. The places where values are lower are locations closer to the buildings, which is normal as the sky view factor is the portion of sky visible when looking upwards.

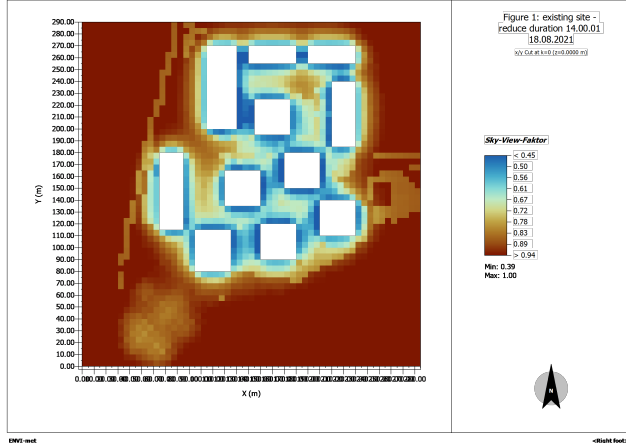


Figure 4: Sky view factor of the site from the simulation

Now, let us take a look at both, air and surface temperatures in the site (respectively Figure 5 and Figure 6). First, we observe some hotter spots on both graphs corresponding to the two adjacent main roads and the large parking lot located at the North-East of the site. This can come from the ground cover material (asphalt and dark concrete pavement) which absorbs a lot of heat. And if we compare the surface temperature with the type of soil (Figure 2), we observe that the hottest locations indeed correspond with these materials.

Looking at the center of the site, we notice a hot-spot with higher air temperature in the North. This area is actually a road with higher traffic than other parts of the site, paved with dark concrete (absorbs a lot of heat). This leads to an issue as the air temperature is exceeding 40°C.

A lower temperature, for both the air and the surface, near the buildings is observed. This can be caused by the shade created by buildings. Additionally, buildings can act as obstructions to various fluxes, thereby altering their patterns. And as we can see on Figure 7, the wind speed is affected by the presence of the buildings. We can see higher speed in the East and West facades and lower in the North and South facades. This wind acceleration can also contribute to the lower temperatures near the buildings by dissipating the heat around the facades. This same trend can also be observed with the relative humidity (Figure 8), where the critical points, with low values, are near the heat-absorbing materials where the experienced temperature will be higher. The vegetated area helps maintain higher relative humidity by promoting moisture retention and evaporation.

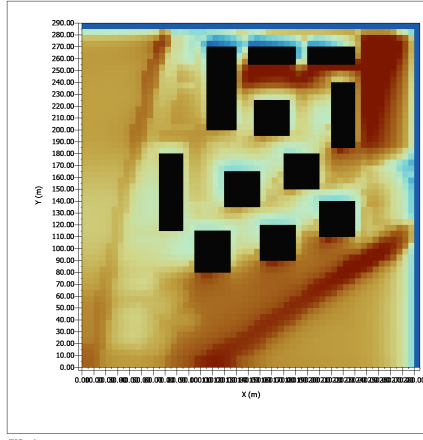


Figure 5: Air temperature [°C]

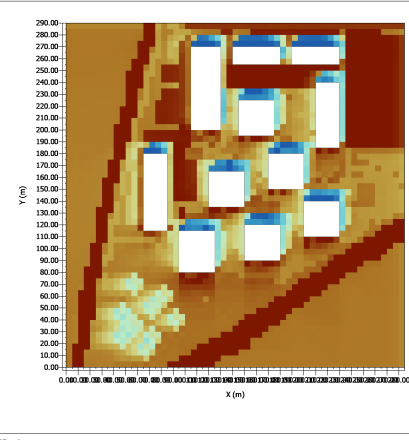
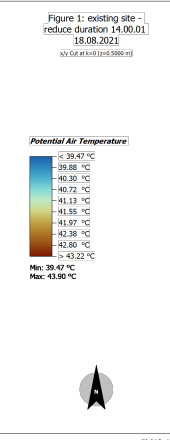


Figure 6: Surface temperature [°C]

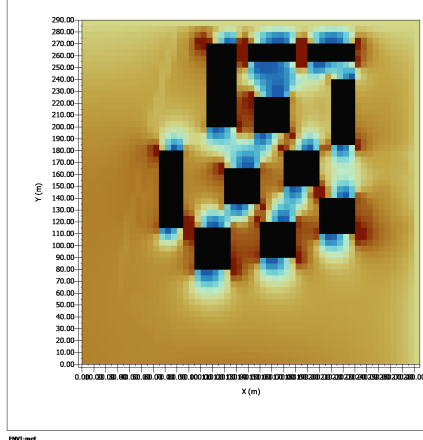
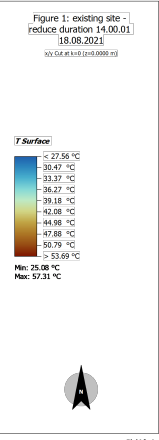


Figure 7: Wind speed [m/s]

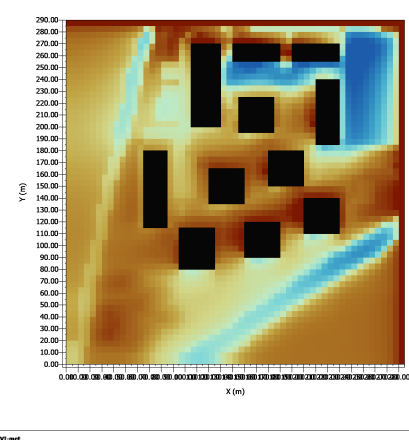
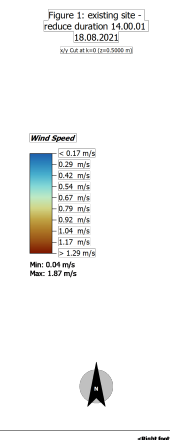
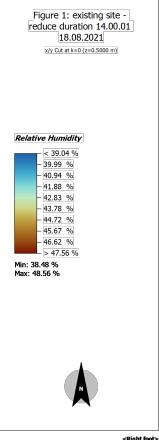


Figure 8: Relative humidity [%]



Regarding the latent heat flux, (Figure 9) we observe that the higher values corresponds to where vegetation is present. This shows that adding vegetation on location of low latent heat fluxes can improve the cooling process through evaporation. Furthermore, lower values correspond to an area with very low evaporative properties (buildings, concrete pavement). For the sensible heat (Figure 10), the observation is the opposite: lower values are for vegetated areas and the highest ones are for heat-retaining materials. Therefore, we can imagine that a possible improvement would seek to increase the latent heat fluxes while reducing the sensible ones. Moreover, the areas that would require these improvement, called hotspots, are the places with high sensible heat and low latent heat flux such as the parking lot, the roads and also at the West of the North-West buildings.

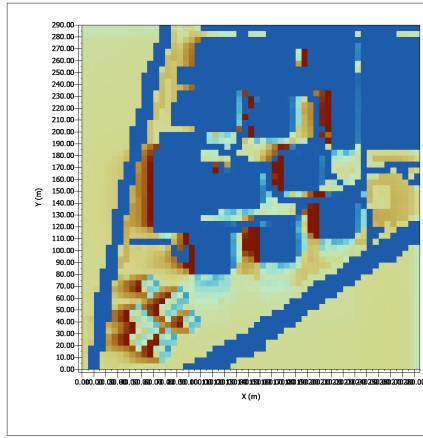


Figure 9: Latent heat fluxes [W/m²]

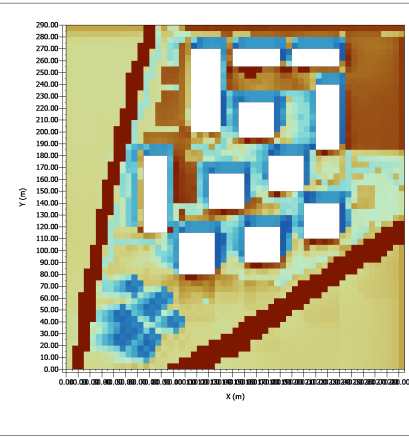
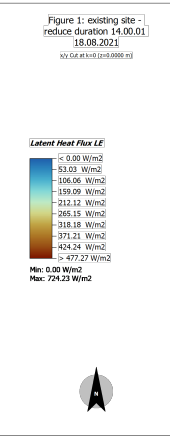
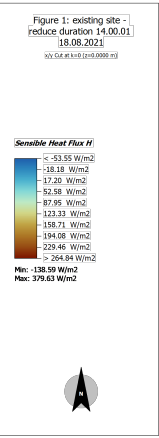


Figure 10: Sensible heat fluxes [W/m²]



Good work on analysis of latent and sensible heat fluxes

If we now look at the reflected shortwave radiation (Figure 11), we can see a clear relation with the surface albedo (Figure 12). In fact, reflected shortwave radiation represents the portion of incoming solar radiation that is reflected back by surfaces. So zones with high values are areas with reflective materials, such as brighter pavement, while low values occur on absorptive surfaces like asphalt or vegetation. These correspond to areas with respectively high and low surface albedo. High values may reduce the phenomenon of heat absorption, but can cause localized warmth due to the reflected heat. Therefore, areas with low reflected shortwave radiation contribute to surface heating, intensifying the urban heat island effect.

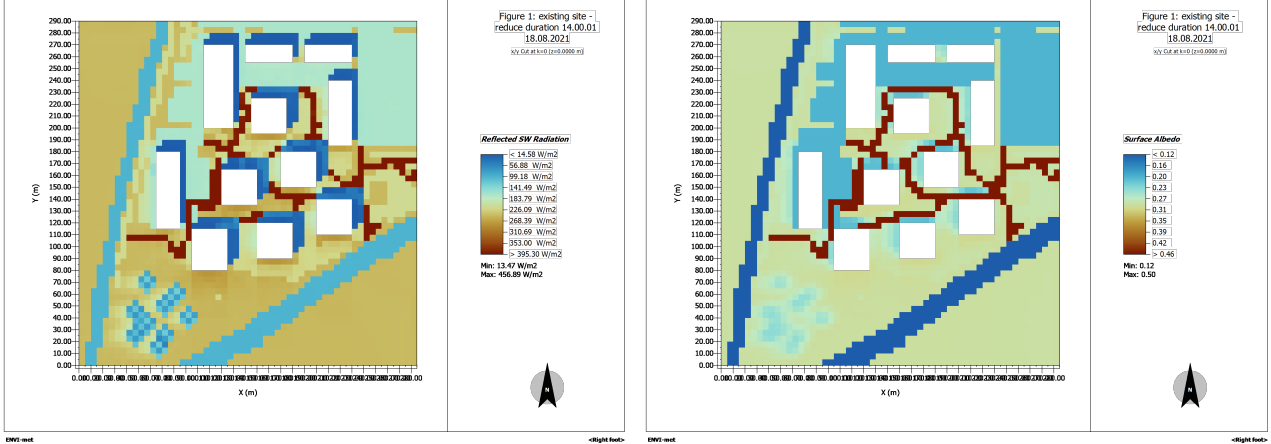


Figure 11: Reflected shortwave radiation [W/m^2]

Figure 12: Surface albedo [/]

We can now take a more in-depth look at our chosen hotspots. We can start by looking at Figure 13 and Figure 14 which respectively represent the surface temperature in $^{\circ}C$ across the day in the middle of the parking lot and in a grass area of the Innovation Park. As we previously observed, the parking lot's surface with dark concrete pavement is hotter but the graph gives an insight of how it varies with time. As we predicted, the choice of material affects the heat release, as the darker concrete will absorb a lot of heat during the hot periods, and will slowly release it when cooling down, while the sandy loam will absorb less heat and it will cool much faster.

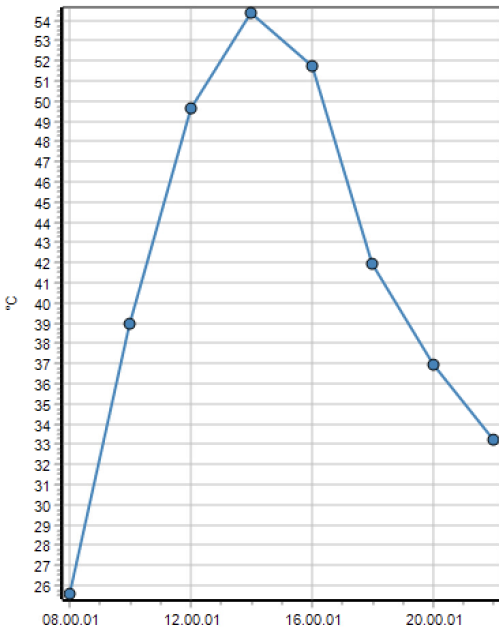


Figure 13: Surface temperature of the parking lot [$^{\circ}C$]

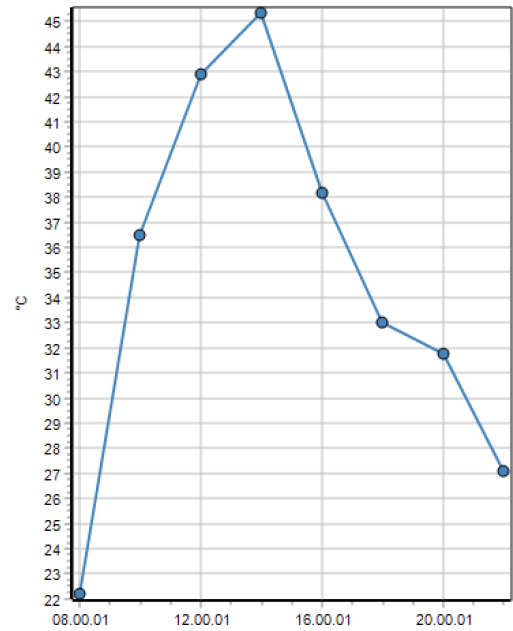


Figure 14: Surface temperature of the grass in the Innovation Park [$^{\circ}C$]

Another hotspot we identified was at the West of the North-West buildings while looking at the latent heat and sensible heat fluxes at this location. We therefore imagined that this zone could have some issues to cool efficiently. If we look at the evolution of the air temperature in this zone (Figure 15), we can notice the issues. It stays at its peak from 2PM to 6PM, so for four hours and then, it starts cooling. And when cooling, it stays

at a relatively high temperature. This can be caused by the surface material used there; the darker concrete pavement, which absorbs a lot of heat and release it slowly, enhances the issue. Another factor could be the lack of obstruction at its West, so in the afternoon, the sun will directly hit the surface.

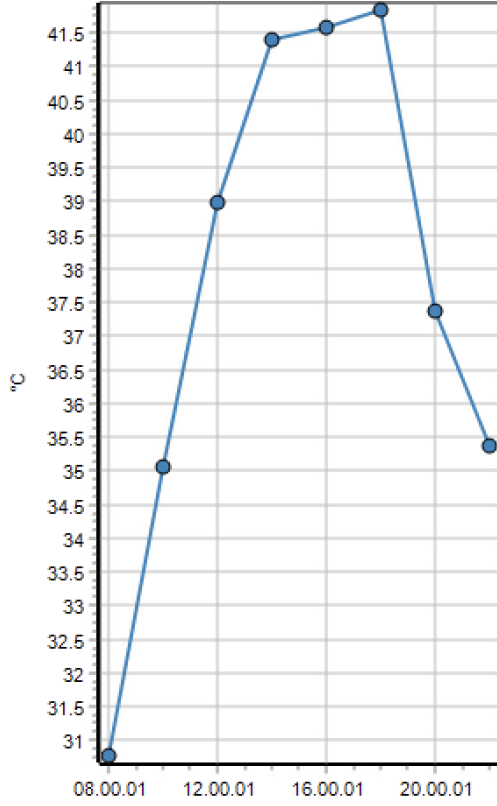


Figure 15: Air temperature at the North-West hotspot [°C]

3 Urban Microclimate Exploration

We will now take a look at the different mitigation strategies in an attempt to find the ones that have the most positive effect on the site in terms of thermal comfort and energy balance. These strategies will be linked with changes in the ground, buildings water bodies and vegetation. To do this we will change a characteristic of the site and proceed with simulations which we will then analyze and compare.

3.1 Ground: Light Concrete

3.1.1 Selected mitigation & hypothesis

Initially, the ground surface consists of a combination of asphalt (for the roads), dark and light concrete, and predominantly sandy loam.

First, we consider the scenario where the dark concrete is replaced with light-colored concrete. This alteration changes the surface's capacity to absorb and reflect solar radiation. Light concrete, with a higher albedo (0.5 compared to 0.2), reflects more sunlight and absorbs less heat. This is expected to result in a lower mean radiant temperature (MRT) in areas with the light concrete. However, given the relatively small area covered by the concrete, the overall impact on air temperature across the park is anticipated to be minimal.

The direct impact is not on MRT.

3.1.2 Simulation results

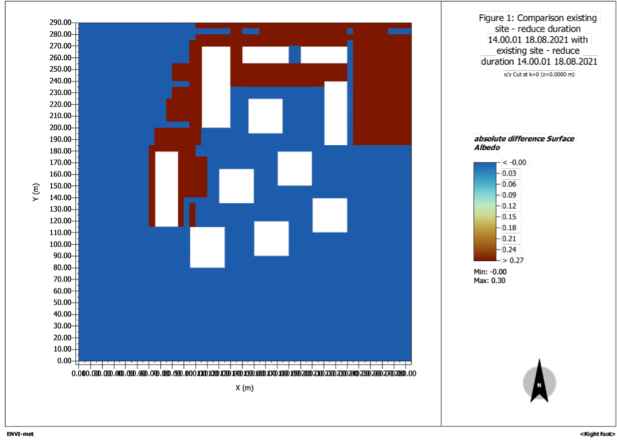


Figure 16: Absolute difference in Albedo

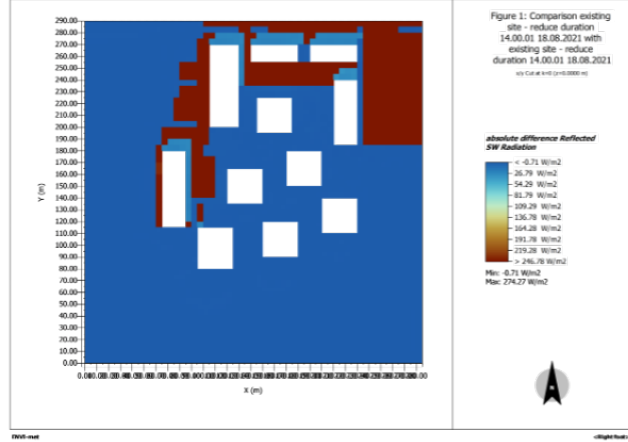


Figure 17: Absolute difference in reflected radiation [W/m²]

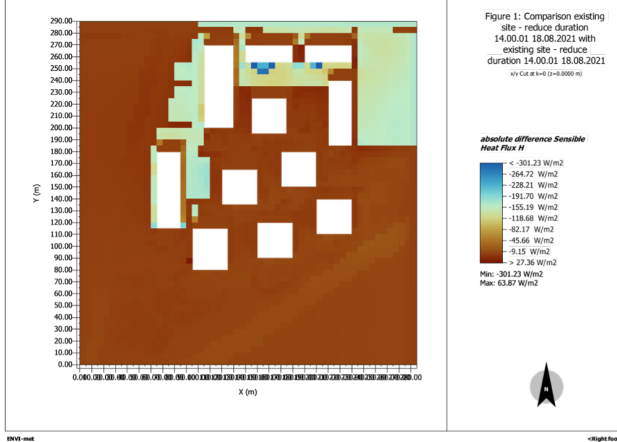


Figure 18: Absolute difference in sensible heat flux [W/m²]

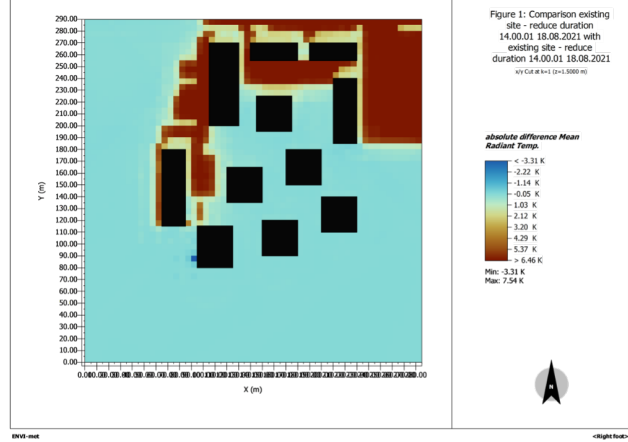


Figure 19: Absolute difference in MRT [K]

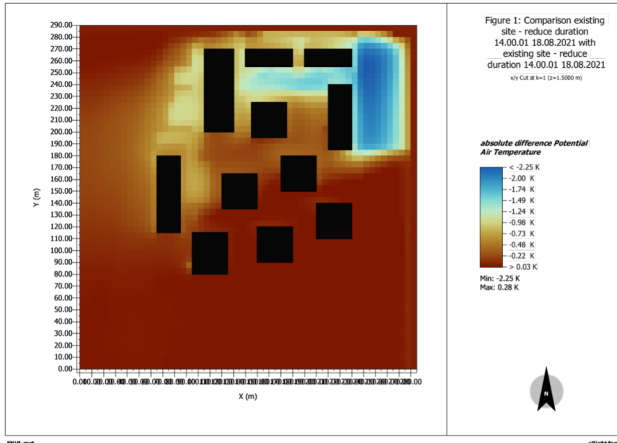


Figure 20: Absolute difference in pot. air temperature [K]

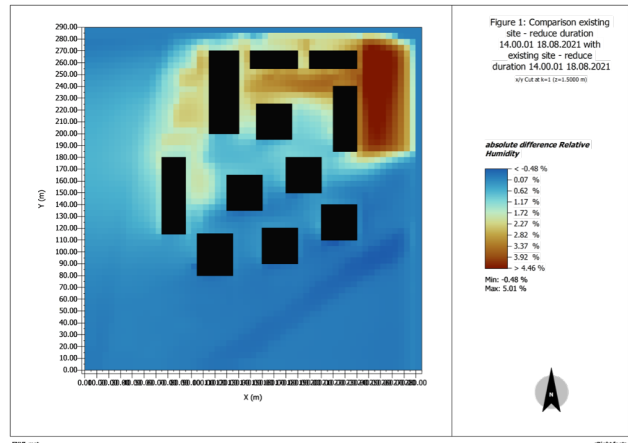


Figure 21: Absolute difference in relative humidity [W/m²]

3.1.3 Discussion

As expected, Figures 16 and 17 illustrate how the implementation of lighter concrete leads to an increase in albedo by 0.27, resulting in a significant rise in reflected radiation.

Figure 18 shows the change in sensible heat flux. It is evident that in the regions where lighter concrete was applied, there is a decrease of approximately 150 W/m^2 . This aligns with our expectations, as sensible heat flux represents the transfer of heat from the surface to the air due to temperature differences, and lighter concrete reflects more solar radiation, reducing surface heating.

Turning to air temperature, we observe surprisingly positive results. Although we anticipated that the limited surface area covered by concrete would have a negligible impact, Figure 20 reveals two noteworthy points. First, there is a significant temperature reduction in the areas where concrete was installed, contrary to our expectations of minor changes mitigated by the surrounding park area. Second, this temperature change extends to neighboring areas, showing a drop of about 1 K around $Y = 200 \text{ m}$. While this decrease may seem modest, when combined with other similar reductions, it can contribute to a substantial overall cooling effect.

However, Figure 19 indicates a marked increase in MRT of approximately 6 K in the areas where concrete was placed. This is likely due to the increased reflected radiation, which significantly influences MRT. Despite the greater rise in MRT compared to the decrease in air temperature, we still consider this mitigation strategy beneficial. The concrete zones are not areas of heavy pedestrian traffic and are unlikely to be used as resting spots by park visitors. Since the MRT increase does not extend to the rest of the park, we believe that in areas of importance, this strategy effectively reduces temperature and enhances thermal comfort.

Finally, Figure 21 shows an increase in relative humidity (RH) of nearly 5% in the regions with the new concrete. While this increase is concerning, it minimally affects the rest of the park. For the same reasons we downplay the MRT increase, we similarly deem the RH increase to be of minor concern, as it does not significantly impact the key areas of the park.

3.2 Ground: Clay Soil

3.2.1 Selected mitigation & hypothesis

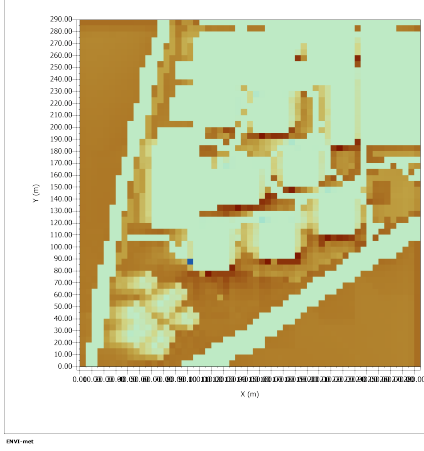
In this scenario, we decided to change the type of ground surface, replacing the original sandy loam with clay soil.

This modification is expected to influence several factors. First, the latent heat flux is likely to increase, as clay soil retains more water due to its higher water-holding capacity compared to sandy loam. Additionally, a decrease in sensible heat flux is anticipated; with more water retained in the clay soil, a larger fraction of the incoming energy is directed toward evaporation rather than heating the air, thereby reducing the sensible heat flux.

Clay soil generally has a slightly lower albedo than sandy loam, meaning it reflects less shortwave radiation. This change is expected to result in a decrease in both the mean radiant temperature (MRT) and air temperature. The increase in latent heat flux, combined with the reduction in sensible heat flux, leads to cooler surface temperatures, further contributing to a cooler environment.

Lastly, since clay soil supports higher evaporation rates than sandy loam, it is expected to result in an increase in relative humidity.

3.2.2 Simulation results

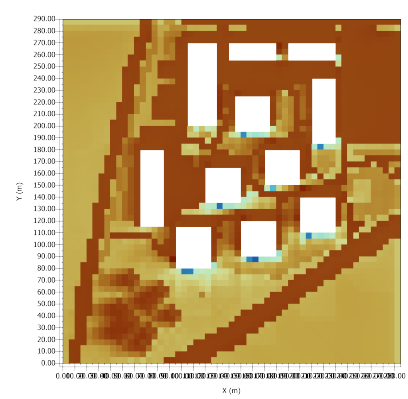


ENVI-net

Figure 1: Comparison existing site - reduce duration
14.00.01 18.08.2021 with
existing site - reduce
duration 14.00.01 18.08.2021
v3 Cut at k=0 (z=0.000 m)

absolute difference Latent
Heat Flux LE

Min: -168.90 W/m²
Max: 252.99 W/m²



ENVI-net

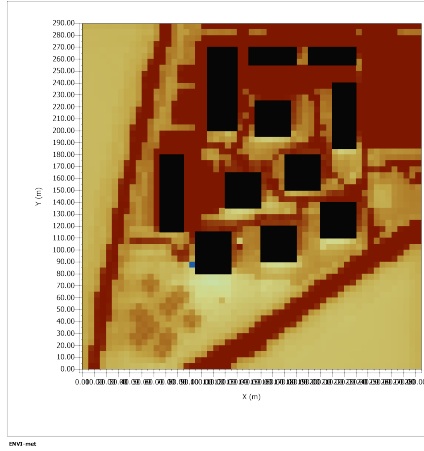
Figure 1: Comparison existing site - reduce duration
14.00.01 18.08.2021 with
existing site - reduce
duration 14.00.01 18.08.2021
v3 Cut at k=0 (z=0.000 m)

absolute difference Sensible
Heat Flux H

Min: -23.60 W/m²
Max: 53.67 W/m²



Figure 22: Absolute difference in latent heat flux [W/m²] Figure 23: Absolute difference in sensible heat flux [W/m²]

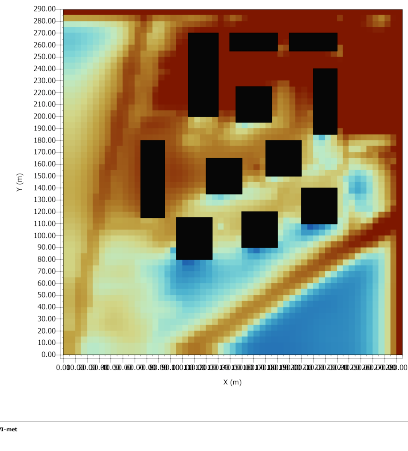


ENVI-net

Figure 1: Comparison existing site - reduce duration
14.00.01 18.08.2021 with
existing site - reduce
duration 14.00.01 18.08.2021
v3 Cut at k=1 (z=1.500 m)

absolute difference Mean
Radiant Temp.

Min: -5.23 K
Max: 0.00 K



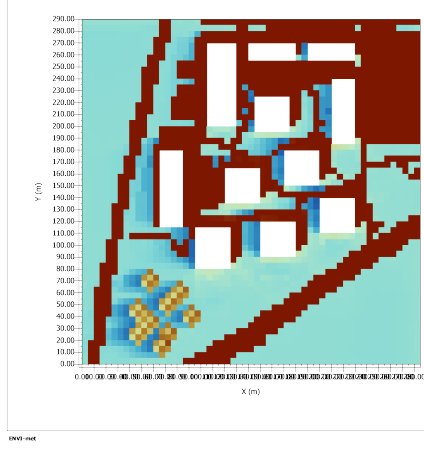
ENVI-net

Figure 1: Comparison existing site - reduce duration
14.00.01 18.08.2021 with
existing site - reduce
duration 14.00.01 18.08.2021
v3 Cut at k=1 (z=1.500 m)



Figure 24: Absolute difference in MRT [K]

Figure 25: Absolute difference in potential air temperature [K]

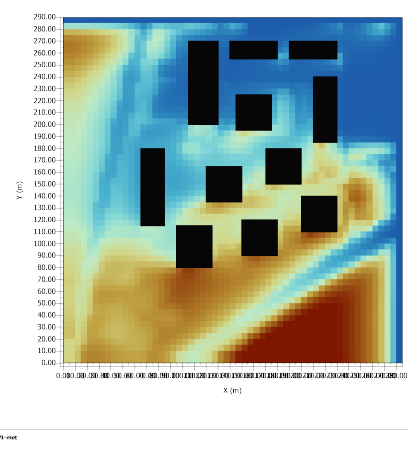


ENVI-net

Figure 1: Comparison existing site - reduce duration
14.00.01 18.08.2021 with
existing site - reduce
duration 14.00.01 18.08.2021
v3 Cut at k=0 (z=0.000 m)

absolute difference Reflected
SW Radiation

Min: -47.90 W/m²
Max: 0.00 W/m²



ENVI-net

Figure 1: Comparison existing site - reduce duration
14.00.01 18.08.2021 with
existing site - reduce
duration 14.00.01 18.08.2021
v3 Cut at k=1 (z=1.500 m)



Figure 26: Absolute difference in reflected radiation [W/m²] Figure 27: Absolute difference in relative humidity [W/m²]

3.2.3 Discussion

As shown in Figure 22, an increase in latent heat flux is observed, as anticipated. This increase is primarily attributed to the water-holding capacity of clay soil. Since clay retains more water, a greater amount of energy is required to convert the retained water into vapor, thus increasing latent heat flux.

Notably, the South sides of the buildings experience higher latent heat flux. This can be explained by the increased exposure to sunlight. South-facing sides of the buildings typically receive the most direct sunlight, especially during the afternoon when solar intensity peaks. This leads to enhanced evaporation of moisture from the soil or vegetated areas, further increasing latent heat flux. In contrast, the North and East sides of buildings often remain shaded for much of the day, reducing the energy available for evaporation.

In Figure 23, it is evident that, in areas without buildings, the available energy is predominantly used for evaporation rather than for heating the air, resulting in a decrease in sensible heat flux. In the building areas, however, the observed change in sensible heat flux is minimal. This can be attributed to two main factors: first, buildings create shaded zones that reduce direct solar exposure; and second, the Urban Heat Island (UHI) effect moderates temperature fluctuations. Buildings absorb heat during the day and release it gradually at night, resulting in less dramatic changes in sensible heat flux.

The south side of the building experiences a higher absolute change in sensible heat flux, as it is more exposed to solar radiation. This allows the building to absorb more heat compared to the other sides. However, this increased heat absorption leads to a slower release of heat due to the thermal properties of the building materials, causing smaller fluctuations in the surrounding air temperature and, consequently, in sensible heat flux.

Despite the change in ground type, Figures 24 and 25 show that the changes in mean radiant temperature (MRT) and air temperature are minimal in the building area. This is likely due to the dominance of the UHI effect, where the heat retention from buildings moderates temperature fluctuations. The thermal mass of the buildings absorbs heat during the day and releases it slowly, preventing significant changes in both air temperature and MRT, even with the alteration in ground type.

In contrast, in the surrounding area, we observe a decrease of approximately -2.5 K , which could significantly improve thermal comfort, particularly during hot summer months. Such a reduction in temperature can help mitigate the discomfort caused by high temperatures, making outdoor spaces more pleasant.

In Figure 26, we observe a slight decrease in reflected shortwave radiation. This can be attributed to the lower albedo of clay soil compared to sandy loam, meaning that it reflects slightly less solar radiation. This can be seen as a positive change in terms of energy absorption, as the energy absorbed by the clay soil may be used for evaporation. This process would lead to cooler mean radiant temperature (MRT) and air temperatures, assuming sufficient moisture is retained in the soil.

In Figure 27, we see that there is practically no change in relative humidity (RH) in the building area. This is likely due to the presence of impervious surfaces, such as roads, which have low moisture retention and limited evaporation. In contrast, in the wider area with clay soil, we observe an increase in RH. This is logical, as clay soil's higher water-holding capacity allows more solar energy to be used for the evaporation of stored water, rather than increasing air temperature. This enhanced evaporation leads to higher moisture content in the air, which raises the relative humidity in the surrounding environment.

Overall, the change from sandy loam to clay soil has led to various changes in latent heat flux, sensible heat flux, temperature, and relative humidity. The most noticeable effects occur in the areas without buildings, where changes in energy fluxes and temperatures are more pronounced. In contrast, the presence of buildings and the UHI effect have helped to moderate these changes in the building areas. Overall, the shift to clay soil has the potential to improve thermal comfort in the surrounding environment, particularly during hot periods, by enhancing moisture retention and evaporation processes.

3.3 Building Alteration: Height

3.3.1 Selected mitigation & hypothesis

Initially, the buildings featured varying heights and footprints. To investigate the impact of these factors, we decided to study the effect of altering both height and footprint configurations.

First, we increased the height of the buildings on the eastern side to reach 25 m which would mean an increase of 3 meters, (\approx one storey) for the highest buildings. The primary goal of this change was to provide additional shading over the park during specific times of the day. We focused on the eastern buildings to ensure shading during the morning hours, aiming to reduce temperatures during peak hours later in the day.

Regarding the results, we primarily expect a reduction in air temperature due to reduced direct solar radiation reaching the ground and surrounding surfaces. For the same reasons, we anticipate a decrease in the mean radiant temperature (MRT), one of our principal measures of thermal comfort. However, we do have a potential

increase of an urban heat island effect (UHI) since we now have larger buildings. Additionally, we expect a slight increase in relative humidity as a secondary effect, resulting from reduced evaporation and plant transpiration. The modifications to building heights are illustrated in Figure 28.

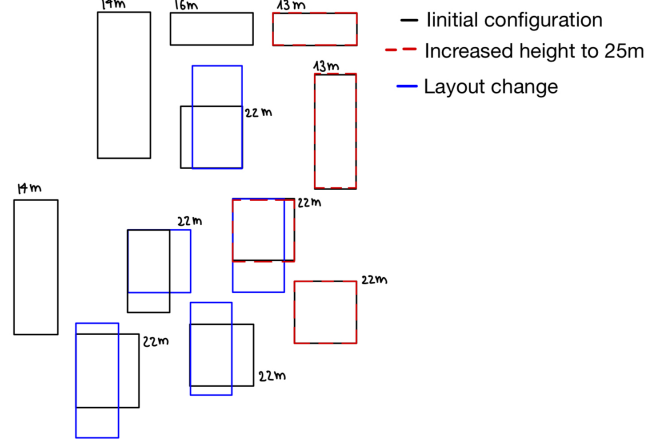


Figure 28: Choice of mitigations strategies for buildings (height and layout)

3.3.2 Simulation results

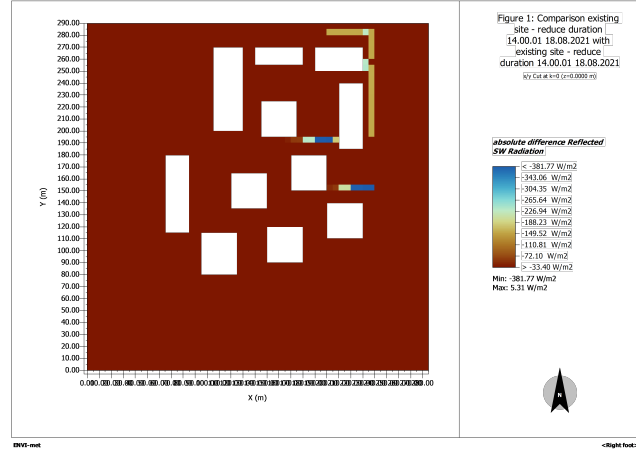


Figure 29: Absolute difference in reflected radiation $[W/m^2]$

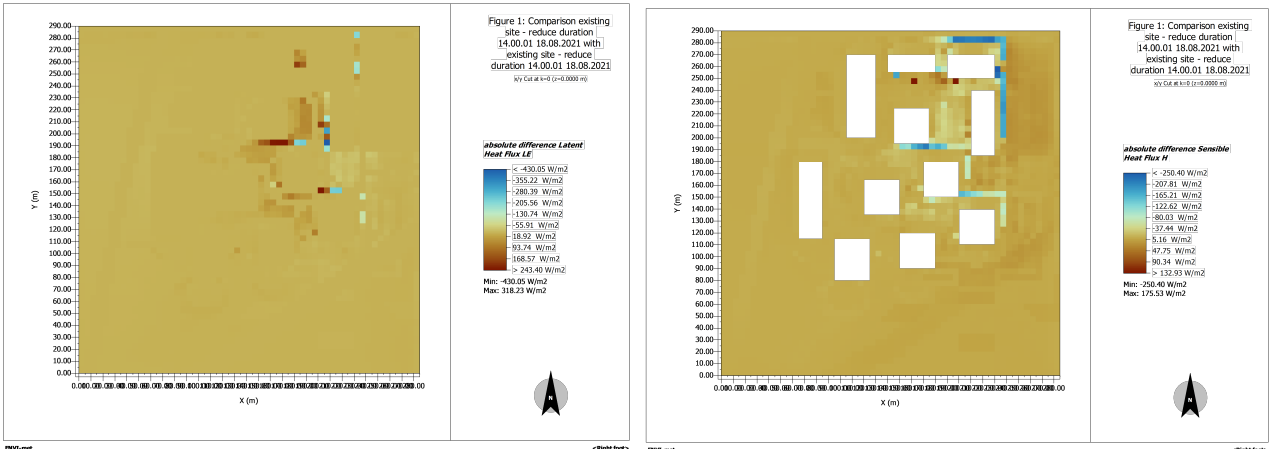


Figure 30: Absolute difference in latent heat flux $[W/m^2]$ Figure 31: Absolute difference in sensible heat flux $[W/m^2]$

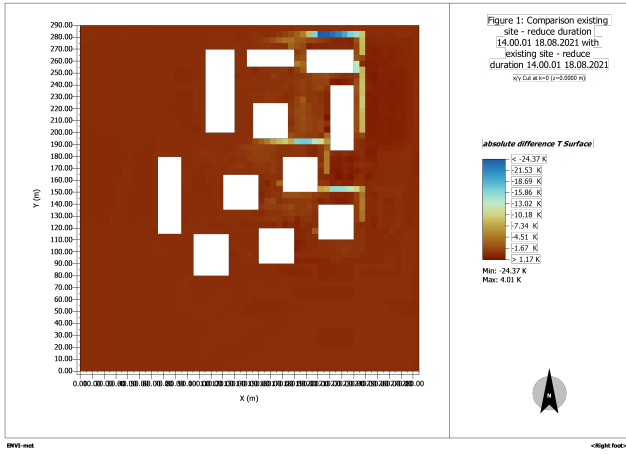


Figure 32: Absolute difference in surface temperature [K]

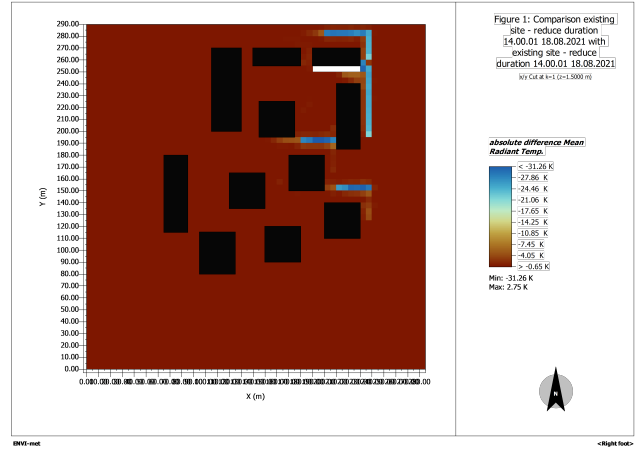


Figure 33: Absolute difference in MRT [K]

3.3.3 Discussion

From examining the results, we immediately identify an error in our initial hypothesis. Initially, we increased the height of the buildings on the eastern side to delay the heating of the surfaces within the park (to the West of the altered buildings), with the aim of keeping them cooler for a longer duration during the hottest times of the day. However, we observe that to the West of the taller buildings, there is little to no change in any of the measured factors.

Conversely, we notice a positive change to the East of the buildings, where the shade falls at this time of day. This observation leads to the preliminary conclusion that it is more effective to provide shade directly at the locations we aim to cool, rather than exposing them to direct sunlight and attempting to delay their heating. In this context, it would be more advantageous to increase the height of the buildings on the western side of the park to provide the necessary shade over the park during the hotter hours of the day.

The difference in reflected radiation shown in Figure 29 illustrates the increased shading. We observe a reduction in reflected radiation extending approximately 5 m around the perimeter of the taller buildings. This additional shading of 5 m is substantial and demonstrates early promising results for the effectiveness of this mitigation strategy.

Examining Figures 30 and 31, we note that any potential temperature changes are primarily due to variations in sensible heat flux, which is significantly lower in the shaded regions. In contrast, latent heat flux shows little to no change. This is expected, as changes in latent heat flux are primarily driven by moisture-related processes, such as evaporation or transpiration, which are not strongly affected by shading alone. However, sensible heat, which involves heat transfer from surfaces to the air, is heavily influenced, as less heat reaches shaded areas. This is corroborated by Figure 32, which shows a substantial decrease in surface temperature, with a reduction of $1.17 - (-24.37) = 25.54$ K around the same perimeter observed in the other results.

To assess thermal comfort, we examine MRT in Figure 33, where, consistent with the surface temperature, MRT decreases significantly in the newly shaded zones.

In conclusion, increasing the height of certain buildings, despite its associated costs, offers tangible benefits in terms of urban thermodynamics. It provides a significant increase in shaded areas, leading to positive effects on thermal comfort within the park. Furthermore, we did not observe any increase of a possible UHI effect which is positive. As previously noted, the primary objective of increasing building height should be to provide shade during the hotter hours of the day, rather than attempting to delay surface heating earlier in the day.

3.4 Building Alteration: Shape

3.4.1 Selected mitigation & hypothesis

As a second scenario to alteration of buildings, we decided to change the shape of certain buildings. Altering the shape of the buildings is anticipated to influence wind speed and direction within the park. Depending on the orientation and geometry of the new shapes, buildings could either block or channel wind more effectively. This

could result in localized increases or decreases in airflow, which would impact thermal comfort and dispersion of heat. The change of shape can be seen on Figure 28. We decided on elongating the buildings in a way to reduce the wind circulation horizontally whilst promoting it vertically to be able to compare both cases. For realism purposes we did this so the volumes of the buildings where kept the approximately the same to ensure they could serve the same tasks they do currently.

3.4.2 Simulation results

You can also show the cross section of the site and the wind velocity to confirm your hypothesis about vertical change of wind.

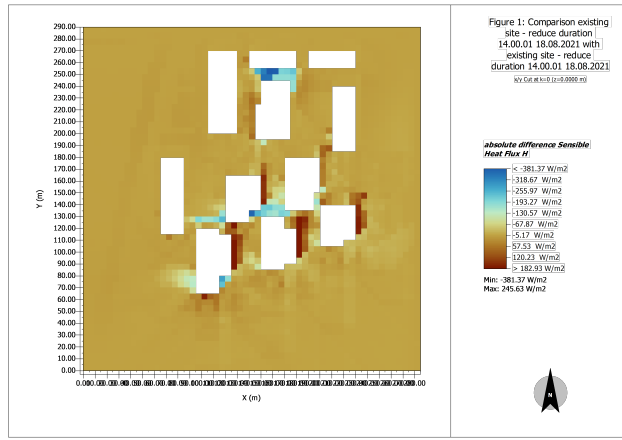
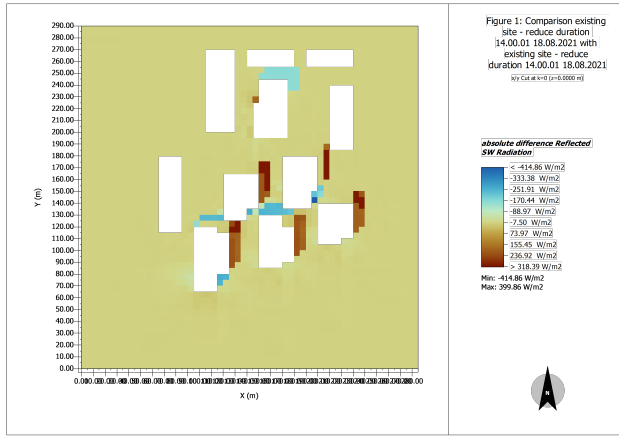


Figure 34: Absolute difference in reflected radiation [W/m^2] Figure 35: Absolute difference in sensible heat flux [W/m^2]

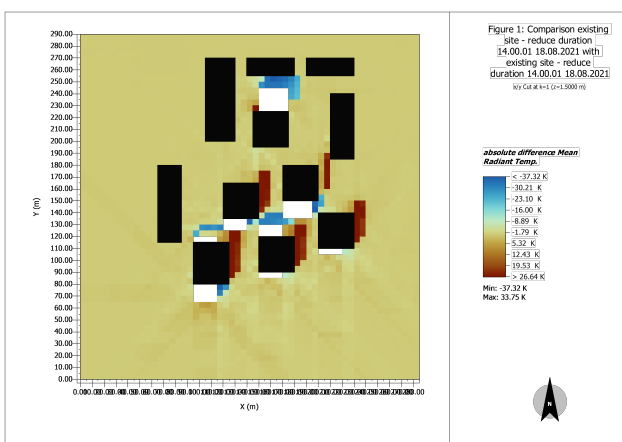
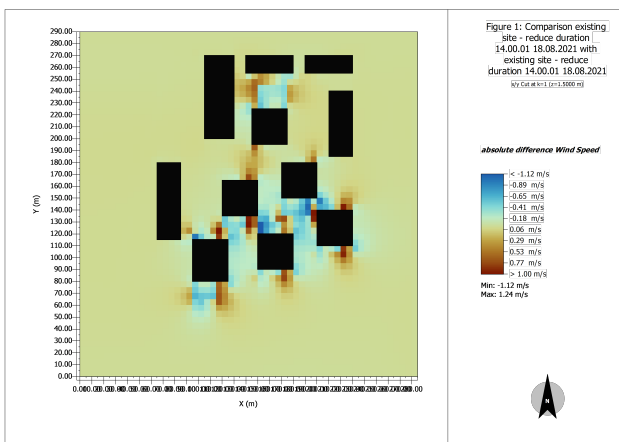


Figure 36: Absolute difference in wind speed [m/s]

Figure 37: Absolute difference in MRT [K]

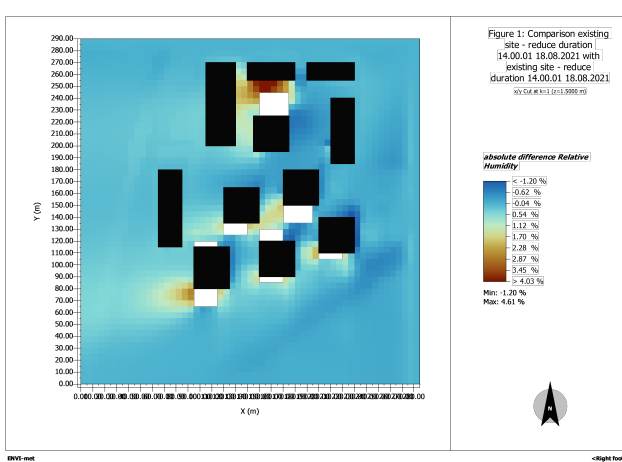
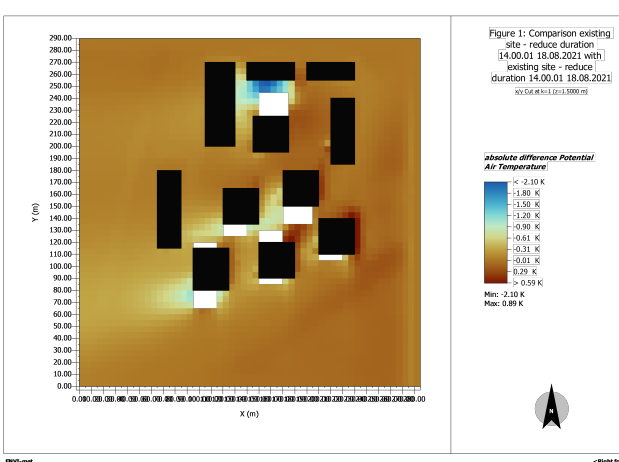


Figure 38: Absolute difference in air temperature [K]

Figure 39: Absolute difference in relative humidity [%]

3.4.3 Discussion

We begin by examining Figure 36, which displays the absolute difference in wind speed and reveals a distinct pattern. The new rectangular buildings tend to experience higher wind speeds along their longer sides (East and West) and lower wind speeds along their shorter sides (North and South) compared to the original square configuration. This phenomenon can be attributed to the longer sides offering a smoother and more continuous surface for airflow, which facilitates faster wind speeds by reducing turbulence. In contrast, the shorter sides create high-pressure stagnation zones where the airflow slows as it encounters the smaller surface areas. These differences in wind flow dynamics emphasize how the rectangular shape disrupts the more uniform wind distribution observed in the original square buildings. Additionally, at a Y-coordinate of approximately 120.00 m, we observe a further reduction in wind speed, caused by the wind being forced to zig-zag between buildings when moving horizontally.

Turning to the air temperature shown in Figure 38, we notice a slight decrease in temperature (approximately 1 K) along the shorter sides of the buildings on the southern part of the park, accompanied by a similarly notable increase along the longer sides. Initially, we anticipated that higher wind speeds would result in more cooling due to increased air circulation. However, this is not the case for several reasons. First, heat dissipates more efficiently in slower-moving air. Moreover, when air flows over a hot surface—such as during summer—a thermal boundary layer forms. This is a thin layer of air near the surface where heat transfers from the surface to the air. Higher wind speeds disrupt this boundary layer, reducing the efficiency of cooling. Finally, slower wind speeds allow for more effective evaporative cooling from vegetation, as corroborated by the relative humidity (RH) data in Figure 39.

It is also worth noting that on the northern side of the park ($Y \approx 250.00$ m), we observe the largest decrease in air temperature, reaching almost 2 K, while the wind speed increases only slightly. This significant temperature reduction appears to be primarily influenced by the change in building shape, which has considerably reduced the space between two buildings in this area. This alteration seems to have resulted in a cooling effect, which we hypothesize is mainly due to the increased shading provided.

Indeed, the reduced spacing between the two buildings now benefits from significantly more shade throughout the day compared to the previous configuration. As discussed earlier, shading has a cooling effect on surfaces by limiting the amount of heat absorbed, as evidenced in Figure 34. This highlights the critical role of shading in mitigating heat and enhancing thermal comfort.

While developing hypotheses for this section and analyzing Figure 34, we realized that the observed temperature changes throughout the park were influenced not only by variations in wind speed but also by alterations in the shading patterns over the park. By examining Figure 34, we noticed that areas with higher reflected radiation corresponded to higher temperatures, while areas with lower reflected radiation exhibited lower temperatures. This observation led us to conclude that the most significant factor contributing to the reduction in air temperatures was likely the shading effect, rather than changes in wind speed.

These variations in air temperature also translate into changes in mean radiant temperature (MRT), as shown in Figure 37. This demonstrates that the proposed mitigation strategy has a tangible impact on reducing the perceived temperatures experienced by park users, thereby enhancing thermal comfort.

In conclusion, this mitigation strategy presents a viable option for increasing thermal comfort within the park. However, it requires careful consideration during the design process. While the strategy can reduce temperatures in some areas, it may inadvertently increase them in others. If not designed properly, this approach could backfire and potentially worsen thermal comfort. This is due to a combination of altered wind speeds and changes in shading patterns, both of which play a critical role.

When compared to the alternative mitigation strategy of altering the heights of the buildings, the results suggest that changing the shapes of the buildings has a greater, albeit similar, impact on temperature reduction. It is also important to note that the specific changes made in this report may not necessarily represent the optimal design choices. Further refinement and optimization are necessary to maximize the effectiveness of this strategy.

3.5 Water Body

In this section, we will study the impact that adding a water body near the site can have on human wellness.

3.5.1 Selected mitigation & hypothesis

In this scenario, the nearest available water body is *Lac Léman*. Although the lake is relatively close to the site, we decided to introduce a water body closer to the site to evaluate its impact on human wellness. In the simulation, this new water body is positioned to the South of the site.

Following the intervention, we expect various positive effects. A water-covered surface influences the energy balance by reducing the sensible heat flux due to its cooling effect, leading to a localized decrease in this flux near the water body. At the same time, we anticipate an increase in the latent heat flux, as the additional water resource enhances cooling through evapotranspiration. Furthermore, since a water surface absorbs more solar radiation than a ground surface, a reduction in reflected shortwave radiation is also expected.

We also foresee changes in relative humidity and the mean radiant temperature (MRT). The presence of a water body is likely to increase relative humidity in the surrounding area due to evaporation, though we believe this change will have minimal impact on thermal comfort in the working area. Additionally, we expect the wind flow pattern to distribute cool air from above the water body into the working zone, contributing to a reduction in MRT.

3.5.2 Simulation results

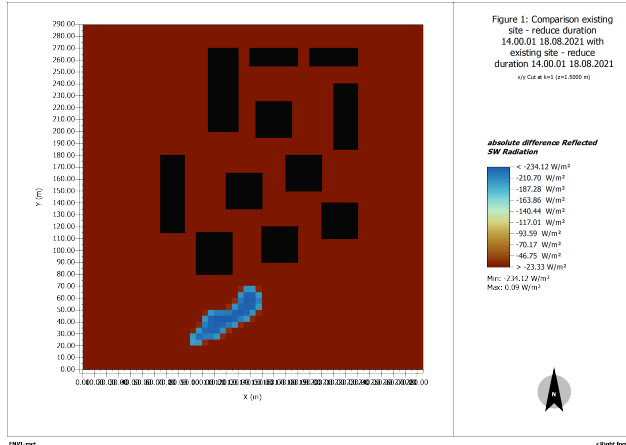


Figure 40: Absolute difference in reflected radiation [W/m^2]

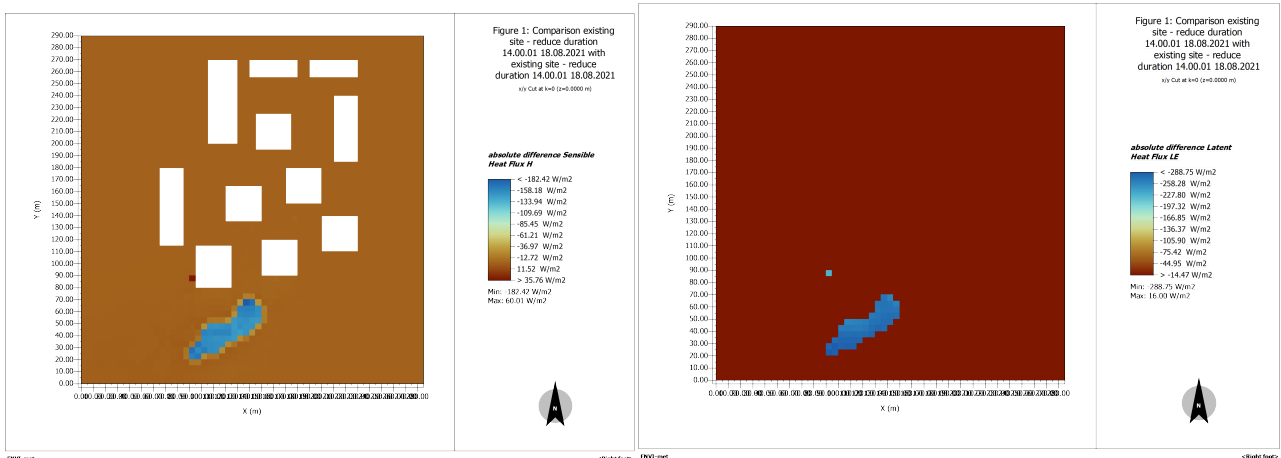


Figure 41: Absolute difference in sensible heat flux [W/m^2] Figure 42: Absolute difference in latent heat flux [W/m^2]

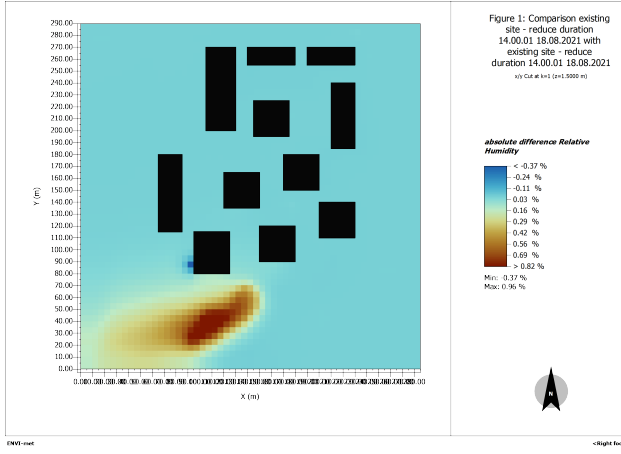


Figure 43: Absolute difference in relative humidity [%]

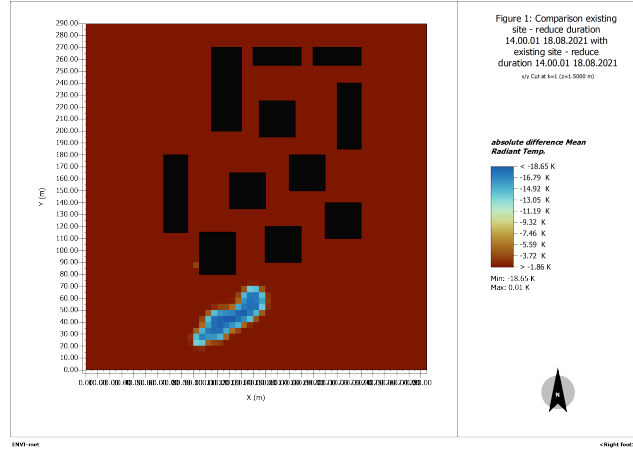


Figure 44: Absolute difference in MRT [K]

What about air temperature? The prevailing wind is from north-east as you analysed, why not put the water pond to north east side to extend the cooling effect to the rest of the site?

3.5.3 Discussion

In Figure 40, we observe that our expectations have been met. There is a decrease of -23 W/m^2 in reflected shortwave radiation around the buildings, indicating that the water body absorbs more solar radiation. This absorption increases the water temperature, contributing to a more stable local microclimate, as water's ability to absorb heat without dramatic temperature increases helps to moderate temperature fluctuations. Additionally, latent heat from evaporation may further affect the local climate, either contributing to cooling or localized warming depending on evaporation rates.

In Figure 41, we observe a significant change in sensible heat flux above the water, approximately -182 W/m^2 . In the building area, the change is around -13 W/m^2 , suggesting cooler conditions compared to the land-only scenario. As the simulation was conducted during the summer, this cooling effect enhances thermal comfort during this period by reducing the heat transferred to the air.

We note a decrease in latent heat flux in Figure 42, which was not expected. Given that the simulation results are visualized at 14:00 in the summer, we anticipated a significant amount of evaporation from the water body, which would lead to an increase in latent heat flux. Several factors might explain the decrease, such as high initial relative humidity or low air temperature. However, the most plausible explanation is a potential error in the simulation.

In Figure 43, we observe that even above the water surface, the increase in relative humidity is minimal. This could be due to the small size of the water body, which does not have a significant impact on the local microclimate.

Finally, in Figure 44, we see that in the building area, there is a decrease in MRT of -1.86 K , which is a notable response for a small water body. The wind pattern aids in transporting the cool air generated by the water body into the surrounding area. During summer, the cooling effect of the water body enhances thermal comfort, as lower MRT generally corresponds to a more comfortable environment.

In conclusion, the addition of a water body near the site had a notable impact on several thermal parameters. The reduction in reflected solar radiation and sensible heat flux indicates that the water body contributed to local cooling, thereby improving thermal comfort. However, the decrease in latent heat flux remains unexplained, suggesting a potential error in the simulation. The increase in relative humidity was limited, likely due to the small size of the water body, while the decrease in mean radiant temperature (MRT) contributed to improved thermal comfort in the surrounding area. Overall, although some results did not meet expectations, the addition of the water body showed a beneficial effect on the local microclimate.

3.6 Vegetation: Surface Greenings

Another factor we decided to take into consideration is vegetation. Indeed, vegetation has certain properties that can have effects on the temperature, energy exchange, and overall thermal comfort among other factors.

3.6.1 Selected mitigation & hypothesis

Vegetation is prevalent throughout most of the site, with much of the ground between buildings covered in grass, bushes, trees, and other greenery. Instead of increasing the amount of vegetation on the ground, which is already substantial and therefore would not have a significant impact on the thermal comfort of the community, we decided to add greenery to the facades and roofs of the buildings. It is important to note that, for our simulation, we placed vegetation on all the facades and roofs. This approach, however, would not be entirely feasible for two reasons. Firstly, the buildings require windows, and secondly, most roofs are already equipped with solar panels. As a result, our simulation results reflect extreme values. If implemented in real life, we should expect a similar effect, however less pronounced.

We expect this intervention to have a positive effect on several aspects. Firstly, we anticipate a reduction in air temperature due to the cooling effect of vegetation. Additionally, replacing materials with higher albedo, such as concrete or steel, which are the current building materials for the facades, will reduce the overall heat emitted from built surfaces. This reduction in temperature will, consequently, help mitigate the Urban Heat Island effect. Furthermore, we also expect an improvement in air quality due to the vegetation's ability to capture particulate matter and absorb gaseous pollutants.

3.6.2 Simulation results

The following figures show the results of the simulations for the absolute differences between the initial case and the one with the added vegetation.

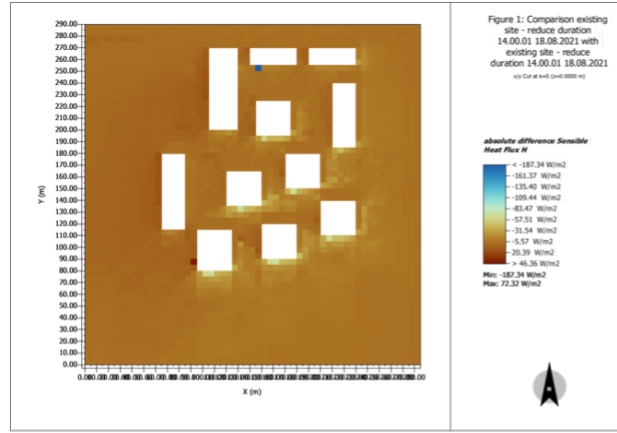
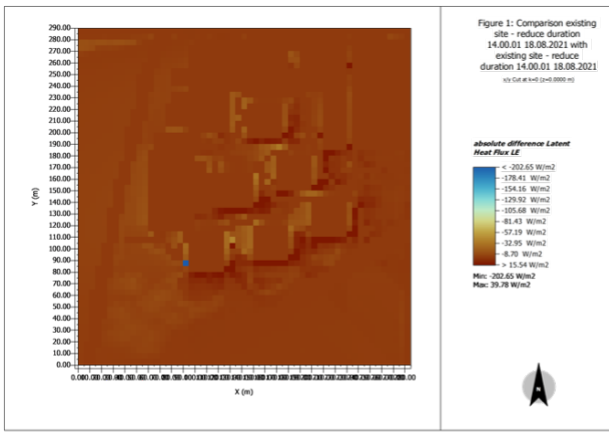


Figure 45: Absolute difference in latent heat flux [W/m²] Figure 46: Absolute difference in sensible heat flux [W/m²]

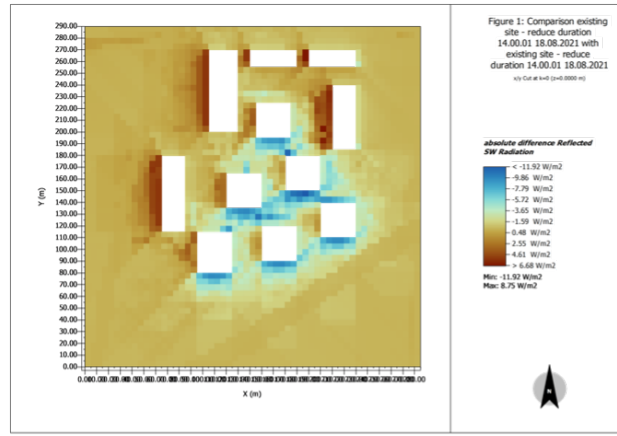
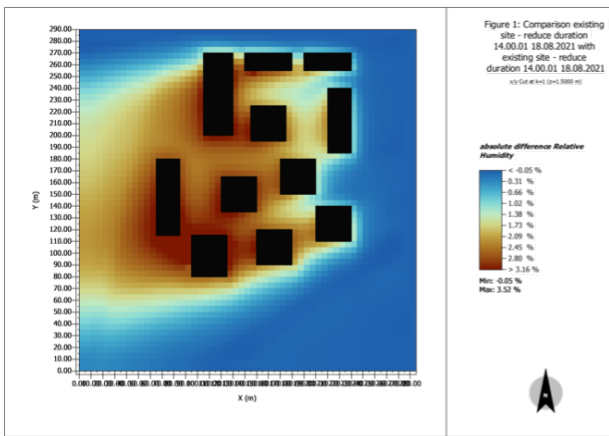


Figure 47: Absolute difference in relative humidity [%] Figure 48: Absolute difference in reflected radiation [W/m²]

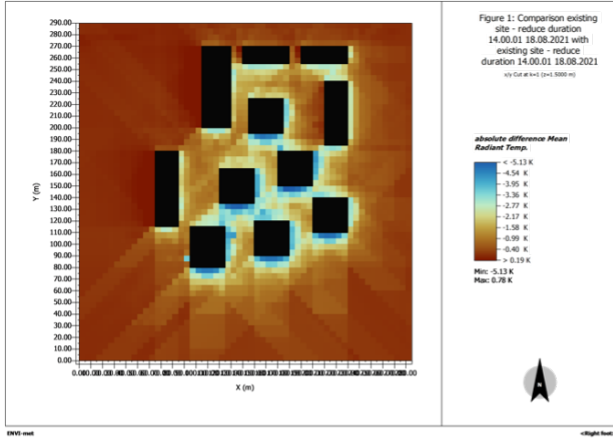


Figure 49: Absolute difference in MRT [K]

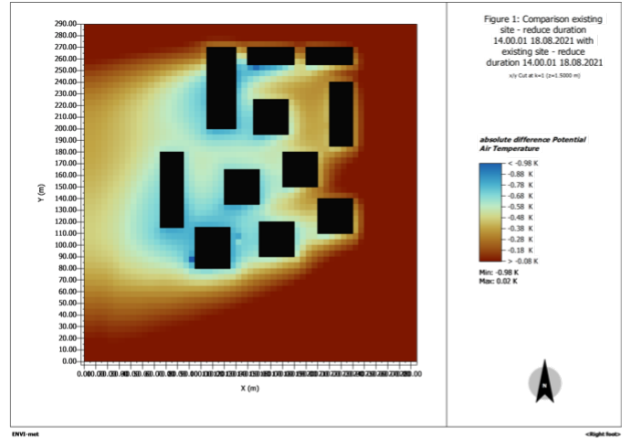


Figure 50: Absolute difference in potential air temp. [K]

3.6.3 Discussion

Firstly, we examine how the addition of greenery on the roofs and facades affects heat flux. Figures 45 and 46 show the absolute difference in latent and sensible heat flux, respectively. We observe that both fluxes increase considerably throughout the entire map. However, this increase is due to an issue where the initial data were much lower than the new simulated data, even in regions where the greenery would not have any effect. Therefore, we will focus on areas where the difference is more or less compared to the rest of the map. For latent heat flux, which is an important factor, higher values indicate more cooling from evapotranspiration, resulting in lower temperatures. This is evident in the map, where we observe higher latent heat flux near the facades. This trend is also reflected in the temperature results, as the temperatures are lower near the facades. A lower sensible heat flux, as seen near the facades, means less heat is transferred into the air, reducing the air temperature. This effect can be seen in the potential air temperature results in Figure 50.

Next, we examine the change in mean radiant temperature (MRT), shown in Figure 49. We immediately notice a significant decrease in temperature of over 5 Kelvin very close to the facades. Furthermore, between buildings, the MRT decreases by 1 to 3 Kelvin, depending on the proximity of the buildings. It appears that the proximity of buildings plays a considerable role in the effectiveness of this mitigation process in terms of MRT. This insight could influence decisions regarding the placement of greenery and whether it is worthwhile to install greenery on more isolated buildings, where the effect may be less pronounced.

Figure 50 reveals some similarities, showing colder air temperatures closer to the facades. However, in this case, we observe the strong influence of wind on air temperature. Even when some buildings are close together, they do not necessarily exhibit lower air temperatures due to wind effects. This observation could further guide the placement of greenery to ensure it is protected from the wind.

Finally, we examine relative humidity in Figure 47. We notice an increase in relative humidity; however, the maximum increase is only 3.16% which we believe is acceptable since the benefits still outweigh this issue.

Next, we look at Figure 48, which shows the absolute difference in reflected radiation. We observe that replacing a higher albedo material with a lower albedo material reduces the amount of radiation reflected, as vegetation absorbs radiation. However, since this radiation is used for natural processes such as photosynthesis, the surfaces are cooled instead of heated.

When we group all the results together, we can analyze the effectiveness of this mitigation method. The reduction in potential air temperature and especially the MRT, are good indicators of thermal comfort and demonstrate how greenery can positively impact the community by cooling air during hot summer days. Although there is a slight increase in relative humidity, which is a concern given that the region already has high humidity levels, the increase is marginal. We believe this is outweighed by the significant temperature reduction provided by this method.

3.7 Vegetation: Removal of Trees

3.7.1 Selected mitigation & hypothesis

In this section, rather than examining the positive impact of trees on thermal comfort, we have chosen to investigate the negative effects of tree removal on the environment. By adopting this perspective, we can better appreciate the measures that have already been taken and highlight the potential impacts of tree removal. Furthermore, the ongoing removal of trees to facilitate urban development is a growing trend. This scenario represents a plausible and realistic case.

We anticipate that this simulation will result in the following negative effects. We believe that the wind flow pattern will be altered, potentially leading to an increase in wind speed. In the absence of the cooling effect provided by trees through evapotranspiration, we expect an increase in sensible heat flux and a decrease in latent heat flux. These changes will lead to a higher mean radiant temperature (MRT) and an increase in shortwave radiation. Furthermore, with no trees to generate evapotranspiration, we expect a decrease in relative humidity.

3.7.2 Simulation results

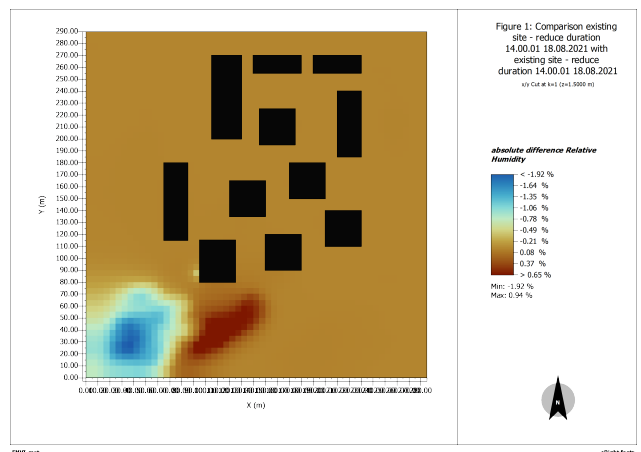
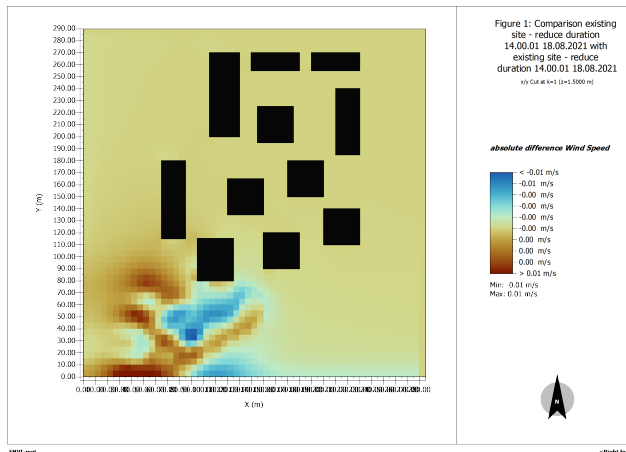


Figure 51: Absolute difference in wind speed [m/s]

Figure 52: Absolute difference in relative humidity [%]

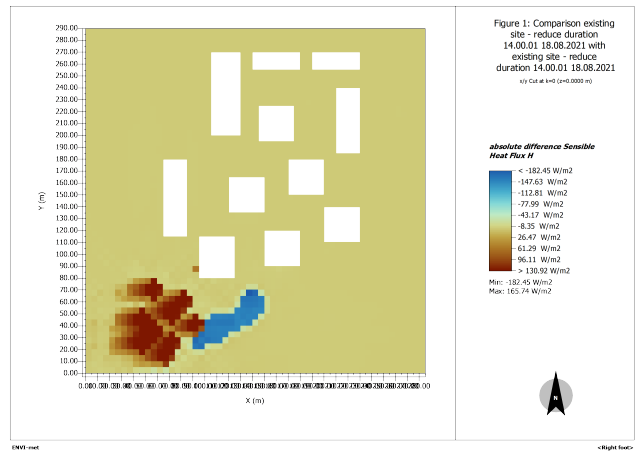
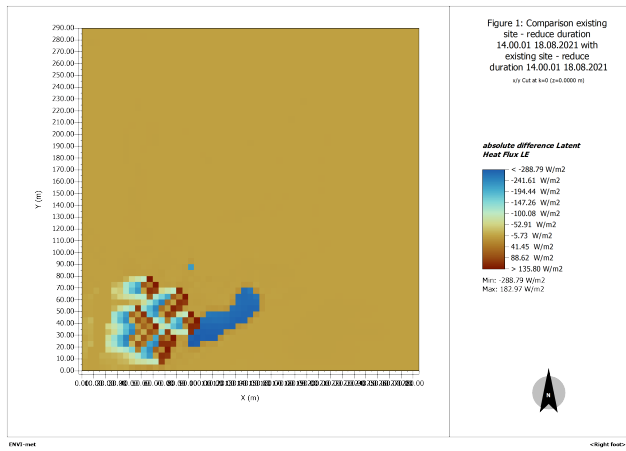


Figure 53: Absolute difference in latent heat flux $[W/m^2]$ Figure 54: Absolute difference in sensible heat flux $[W/m^2]$

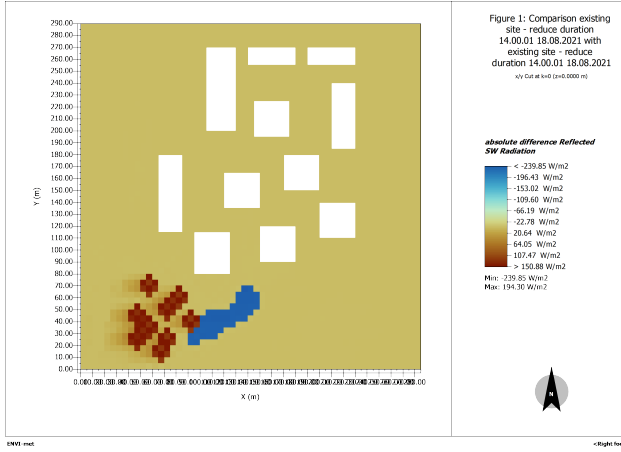


Figure 55: Absolute difference in reflected radiation $[W/m^2]$

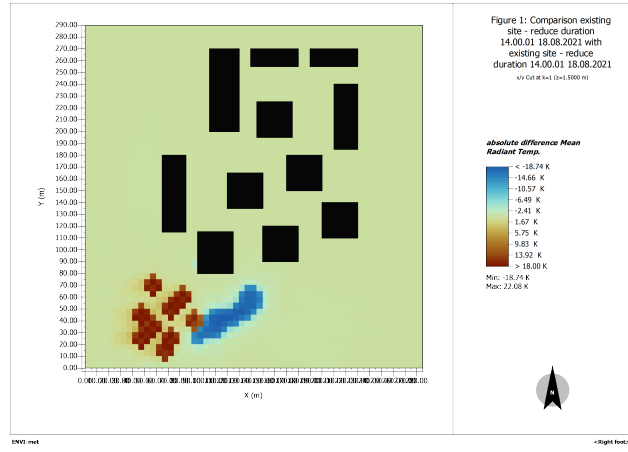


Figure 56: Absolute difference in MRT [K]

3.7.3 Discussion

Firstly, we observe that in each simulation, a water body appears to be near the area where trees were removed. Despite verifying the initial conditions multiple times, this issue persists, while the program indicating that no water body is present. For the purposes of our analysis, we will disregard the minor effects of this imaginary water body.

Secondly, in Figure 51, no significant change in wind speed is observed. This can be attributed to the fact that only a few trees were initially present, and their density was insufficient to influence wind speed. During our site exploration, we noted that the area contained only a small number of trees relatively small, rather than a dense forest.

Then, in Figure 52, we observe a decrease in relative humidity of approximately -1.8% in the area where trees were removed. However, near the buildings, there is practically no change in relative humidity. As previously mentioned, the area initially contained only a small number of trees, whose contribution to evapotranspiration and local moisture levels was likely minimal. Consequently, their removal does not significantly affect relative humidity overall, but only locally. Furthermore, the surrounding environment is dominated by impermeable surfaces, such as asphalt and concrete, which limit any noticeable change in atmospheric moisture content.

To continue, in Figures 53 and 54, the absence of trees leads to a significant reduction in latent heat flux in the area where the trees were removed, as the trees no longer contribute to evapotranspiration. This results in less moisture being released into the air, diminishing the cooling effect that would otherwise help moderate the temperature. Simultaneously, without trees, the surface becomes more exposed to solar radiation, causing the ground temperature to rise. As a result, sensible heat flux increases, transferring more heat to the air, which makes the environment hotter.

The minor changes in sensible and latent heat flux near the buildings after tree removal can largely be attributed to the Urban Heat Island (UHI) effect. In urban environments, the UHI effect plays a significant role, as built-up areas like roads and buildings absorb and retain heat much more than surrounding rural areas. Therefore, the removal of trees, which would typically provide cooling through evapotranspiration, has a relatively minor impact on the already warm microclimate near the buildings.

Furthermore, in Figure 55, the removal of vegetation results in an increase in reflected shortwave radiation. This indicates that the trees were replaced by high-albedo materials, making the surface more reflective after the tree removal. These surfaces typically reflect more solar radiation compared to vegetation, which absorbs a significant amount of radiation. As a result, reflected shortwave radiation increases up to $194 W/m^2$. Since the forest density was low, no significant change is observed in the building area.

Finally, in Figure 56, the primary change is an increase in mean radiant temperature (MRT) by $18 K$ in areas previously shaded by trees. This increase is due to increased exposure to solar radiation and the loss of cooling from evapotranspiration. The resulting rise in MRT leads to a warmer microclimate and reduced thermal comfort, particularly in areas close to where the trees were removed. However, no significant change is observed in the building area.

In conclusion, the removal of trees significantly impacts local microclimates by reducing evapotranspiration,

increasing sensible heat flux, and altering the energy balance. However, the effects on the building areas are relatively minor. This is primarily due to the low density of the forest in the area, which meant that the trees' contributions to the local microclimate were limited. The most noticeable impacts were observed in areas directly affected by tree removal, with the surrounding environment showing only minor changes.

4 Integrated Microclimate Solution

Now that we have explored changing multiple parameters on our site, we can implement an integrated solution demonstrating multiple mitigation strategies on the microclimate and compare it to the base case. Let us first note that as for the previous analysis, the right bottom corner on the map that is just after the road is not taken into account as it is a private land that is not EPFL property.

The following figure shows a 3D model of the integrated microclimate solution:



Figure 57: 3D model of the integrated microclimate solution.

First, we decided to change the soil of the base case from dark concrete to a light concrete and the sandy loam to clay. As mentioned in 3.1, light concrete has a higher albedo than dark concrete (0.5 compared to 0.2), which means the soil reflects more sunlight and absorbs less heat. As explained in Section 3.2, clay soil retains more water due to its higher water-holding capacity compared to sandy loam. This allows a better thermal comfort than sandy loam overall.

Then, from Section 3.3, we concluded that increasing the buildings' heights was beneficial due to the shading effects. And since, the latter would be more accentuated if the increase was applied to the buildings on the left side of the map, that is what we implemented.

Finally, due to its local shading, low reflective and evapotranspiration properties, we decided to implement trees and grass above clay soil. We paid attention to leave the paths unobstructed and put some trees even between buildings as it is not bothering and rather pleasant to the eye of the people working inside.

4.1 Simulation results

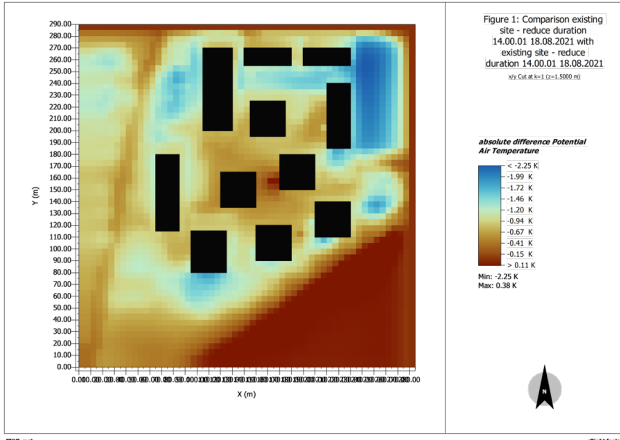


Figure 58: Comparison existing site - reduce duration
14.00.01 18.08.2021 with
existing site - reduce
duration 14.00.01 18.08.2021
y/z Cut at k=1 (z=1500 m)

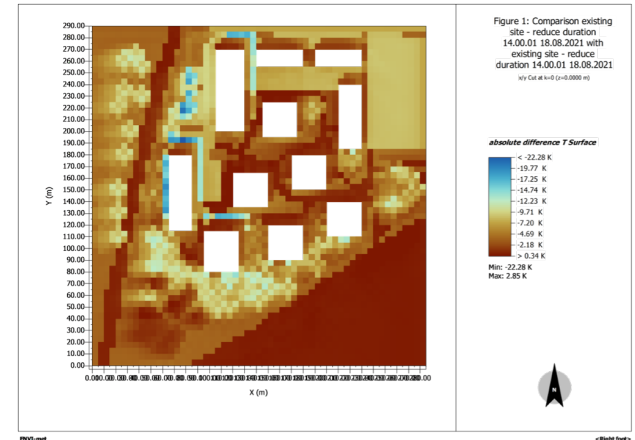


Figure 59: Comparison existing site - reduce duration
14.00.01 18.08.2021 with
existing site - reduce
duration 14.00.01 18.08.2021
y/z Cut at k=0 (z=0.000 m)

Figure 58: Absolute difference in potential air temp. [K]

Figure 59: Absolute difference in surface temp. [K]

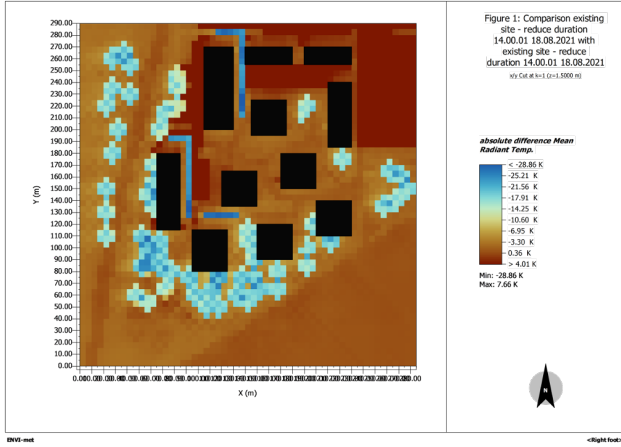


Figure 60: Absolute difference in MRT [K]

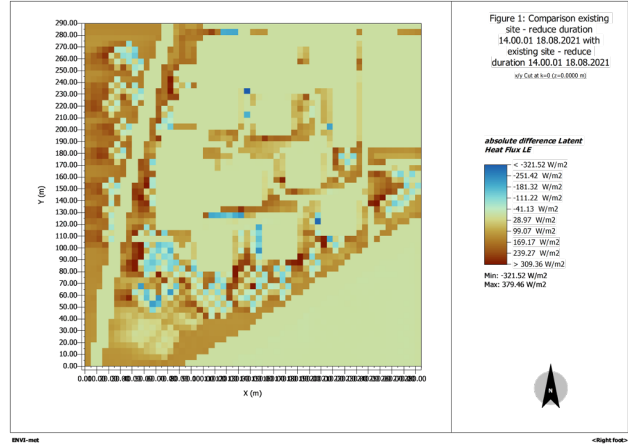


Figure 61: Absolute difference in latent heat flux [W/m^2]

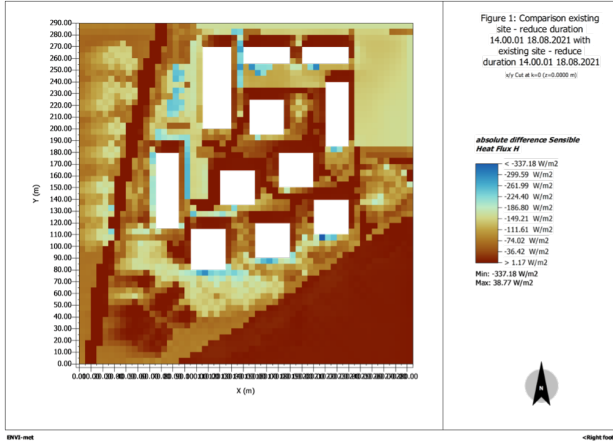


Figure 62: Absolute difference in sensible heat flux [W/m^2]

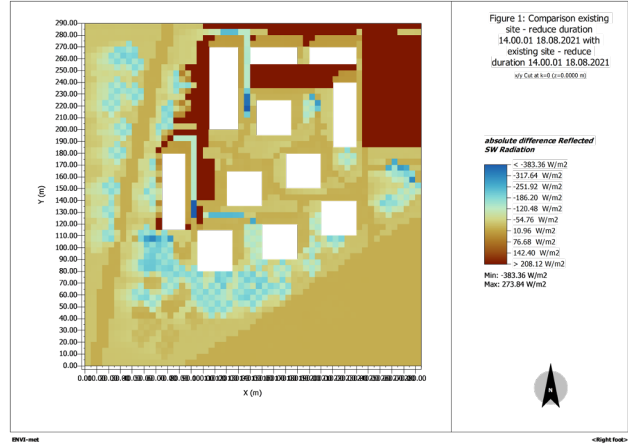


Figure 63: Absolute difference in reflected radiation [W/m^2]

4.2 Discussion

Firstly, we can observe in Figure 58 that the potential air temperature decreases overall by about -1K on the site. The maximum difference is observed in the North-East of the area with -2.25K due to the change in ground to light concrete. Then, looking at Figure 60, we can note that, where trees have been added, the mean radiant temperature drops to around -21.5K. Moreover, we can clearly see in the figure that the temperature decreases almost to -30K, the provided shading following the building's shape. Nonetheless, there is a temperature increase of 4K to 7.6K approximately, where the ground material was changed to a light concrete. This is explained by the increased reflected radiation (see Figure 63), which significantly influences MRT, though it is not a problem as those areas are not of heavy pedestrian traffic.

Further, on Figure 59, we can notice that the surface temperature decreases almost everywhere, most of the areas showing -4.7K to -9.7K temperature differences. Indeed, the temperature difference reaches around -9.7K to -12.2K where the trees were planted and the ground was changed to a light concrete, and -14.7K to the maximum, -22.28K, from the shading of the higher buildings. Nevertheless, the increase in temperature is maximum 2.85K, located on the road (South to West) and connecting the buildings, which is minor compared to the overall great decrease we obtained.

Let us now take a look at the latent and sensible heat fluxes, respectively Figure 61 and 62:

- Latent Heat Flux:

Overall, a positive change in latent heat is observed. This means that overall, more energy is being used for evapotranspiration, which is coherent, since we added more vegetation. This results in higher moisture availability, indicating an increase in cooling. This is a satisfactory outcome in urban climate mitigation. However, we do note some very local negative changes scattered around the center of the site, but these represent a small portion of the site, meaning it does not surpass the positive effect.

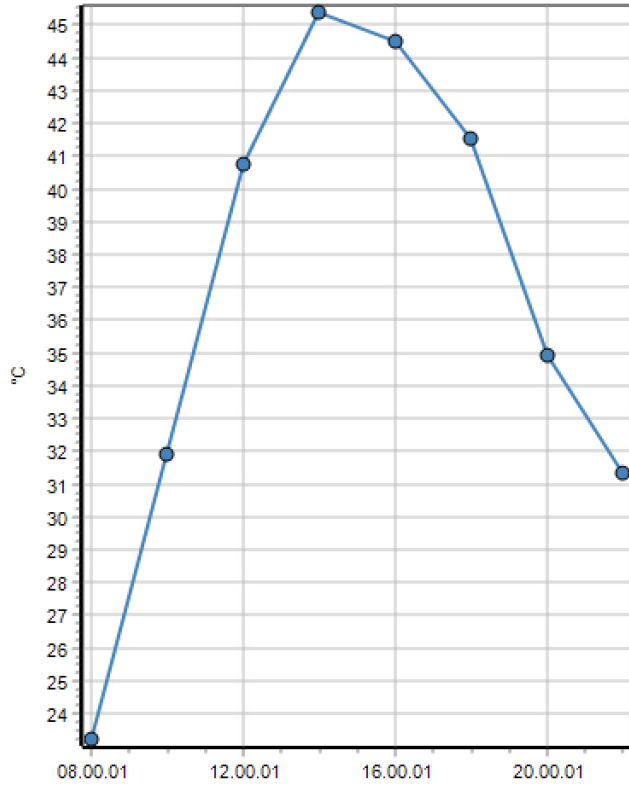


Figure 64: Evolution of the surface temperature in the parking lot [°C]

- Sensible Heat Flux:

We note some specific surfaces with a small (\approx greater than 1.17 W/m^2) positive increase. These surfaces correspond to the road leading from South to North and the pavement in the center of the site. These locations aside, the changes in sensible heat flux are negative, which is beneficial. Indeed, this means that less energy is being transferred as heat, suggesting a cooling effect. Note, that, while the maximum positive change is 38.77 W/m^2 , it matches the smaller negative changes (-36.42 W/m^2). The maximum negative change is -337.18 W/m^2 , which confirms that the cooling effect of this mitigation is much more important than the increased heat at some locations.

Last but not least, let us take a look at the same graph as Figure 13 (displayed in Section 2.3), considering the final mitigation (see Figure 64):

This confirms the satisfactory results of our final mitigation. Indeed, the *shape* of the evolution did not change much, but it shifted to smaller temperatures. The peak temperature dropped from $54.6 \text{ }^{\circ}\text{C}$ (Figure 13) to $45.6 \text{ }^{\circ}\text{C}$ (Figure 64), which is a significant change.

5 Conclusion

In conclusion, this study has provided a comprehensive thermal analysis of the Innovation Park design. To summarize what has been done, first an analysis of the current site design has been done. Using ENVI-met and analyzing a series of performance factors, the results revealed significant flaws in terms of thermal comfort and energy balance. The first hypothesis was due to a lack of vegetation, and the choice of heat absorbing materials, which contributed to the formation of hotspots, with extreme values in critical zones. Based on these findings, several mitigation strategies were proposed by modifying key urban elements. Each strategy was then analyzed individually to understand their impact. By combining the most positive changes observed a global mitigation strategy was then developed which successfully met the expectations for improving the site's thermal behavior.

This study emphasizes the significant impact of urban elements regarding the thermal performance of a city. Even relatively small modifications to a specific feature can lead to substantial changes, both positive and negative, highlighting the importance of considering these factors in urban planning. Therefore, their influence should not be underestimated, especially during critical events such as heatwaves.

For further studies and more in-depth analysis, additional data about the site could be collected, particularly regarding the heat fluxes produced by the buildings in the Innovation park. The surrounding areas should also be considered for their potential impact on the site. Furthermore, to achieve more precise results, a more complex model could be developed. However, the technical limitations of computers and software should be taken into account if this approach is chosen.

6 Annex

6.1 Visit of the site

Location	Natural elements	Ground cover material	Surrounding building material	Surrounding building height	Anthropogenic heat source	Aspect ratio	Sky view factor	Shading sources
A	Bush : + / - Gravel : + Flower : -	Gravel Concrete Grass	Concrete Glass Steel Bricks	16	Car (parking) Human Electric lights	None	≈ 1	Buidling Trees
B	Bush : + / - Grass : + / - Small tree : -	Concrete Grass	Concrete Glass Steel	17	Car (street) Human	17/15 $\approx 1,13$	0,9	Buildings
C	Bush : ++ Grass : - Tree : +	Concrete Grass	Concrete Glass Steel	14	Car (parking) Human	None	0,95	Buildings Trees
D	Bush : + + + Grass : ++ Gravel : + / - Big tree : 2	Sand / soil Concrete Grass	Concrete Glass Steel	14	Human	None	0,96	Buildings High bushes Trees
E	Bush : - Grass : + + Tree : +	Concrete Grass (+ +)	Concrete Glass Steel	20	Human	20/30 $\approx 0,67$	0,7	Buildings
F	Bush : + Grass : + + Tree : -	Gravel Grass	Concrete Glass Steel	20	Human	20/40 $\approx 0,5$	≈ 1	Buildings Tree Stairs strucure
G	Bush : - Grass : + Tree : -	Cement Grass	Concrete Glass Steel	21	Human Car	None	0,9	Buildings Overhang Trees

Figure 65: Data collected during the site visit

6.2 Model of the site

Layer	Wall			Roof		
	1	2	3	1	2	3
Material	Prefabricated concrete wall	Insulation	Plaster	Gravel	Insulation	Reinforced concrete slab
Thickness [m]	0,14	0,1	0,047	0,05	0,2	0,3

Table 1: Materials of each layers for buildings A

Layer	Wall			Roof			
	1	2	3	1	2	3	4
Material	Plaster	EPS expanded polystyrene	Plywood (heavyweight)	Gravel	XPS extruded polystyrene CO2 blow	Concrete reinforced with 2% steel	EPS expanded polystyrene
Thickness [m]	0,01	0,18	0,14	0,1	0,2	0,3	0,065

Table 2: Materials of each layers for buildings B

Layer	Wall			Roof		
	1	2	3	1	2	3
Material	Fiber cement board	Sandwich panel mineral wool	Aluminum	Gravel	Mineral wool insulation	Reinforced concrete slab
Thickness [m]	0,008	0,15	0,002	0,04	0,08	0,35

Table 3: Materials of each layers for buildings C